Journal of Power Sources 196 (2011) 7609–7615

Contents lists available at ScienceDirect

Journal of Power Sources

journal homepage: www.elsevier.com/locate/jpowsour

Design and fabrication of a magnetic fluid micropump for applications in direct methanol fuel cells

Shi-Min Lee[a], Yean-Der Kuan[b,*], Min-Feng Sung[c]

[a] Department of Aerospace Engineering, Tamkang University, 251 Tamsui, Taiwan
[b] Department of Refrigeration, Air-Conditioning and Energy Engineering, National Chin-Yi University of Technology, 411 Taichung, Taiwan
[c] Department of Mechanical and Electro-Mechanical Engineering, Tamkang University, 251 Tamsui, Taiwan

ARTICLE INFO

Article history:
Received 28 February 2011
Received in revised form 26 April 2011
Accepted 27 April 2011
Available online 4 May 2011

Keywords:
Direct methanol fuel cell
Micropump
Magnetic fluid
Portable
Rotary disc
DC motor

ABSTRACT

Direct methanol fuel cells (DMFCs) are widely considered to have great potential for portable electric applications, and the power requirements for many of them are only a few watts. Therefore, a low power liquid pump is especially desirable for driving the methanol solution fuel for an active direct methanol fuel. The main objective of this paper is to design and fabricate a magnetic fluid micropump that has characteristics of low operation voltage and current and is suitable for use in DMFCs. Two prototypes were developed and tested. The magnetic fluid micropumps are successfully applied to drive the fuel to a DMFC, and measurements of the cell performance are also conducted.

1. Introduction

The direct methanol fuel cell (DMFC) uses a methanol solution as fuel. Methanol is a readily available and low-cost fuel source, which has higher volumetric energy density than hydrogen. In addition, the DMFC has the main advantages of near-room-temperature operating conditions, safety, low cost of fuel, quick and convenient refueling, silence, ease of storage and carrying, and conversion of methanol directly into electricity without a bulky reformer. Thus, the DMFC is particularly suited for compact design. One of the most promising short term uses would be in portable applications that only need small amounts of power but high energy density, such as in third-generation (3G) cell phones, high specification person digital assistants (PDAs), and digital movie cameras. DMFC systems are attractive candidates to replace Li-ion batteries due to recent advances in the minimization of DMFC stacks [1,2].

The applications for small portable 3G products such as PDAs, cell phones, and MP3 or MP4 players are suitable for DMFCs because the power required for those products is in the range of a few watts and the power output of DMFCs is also low. For low-power DMFCs, there are two considerations for the liquid fuel feed: passive (pumpless) or active (with pump). The main characteristic of a passive DMFC system is that no pumping and no external power sources are needed. Therefore, many studies have been published on passive DMFCs in recent years, which have been investigated from different aspects, such as optimal fuel concentration, membrane thickness, fabrication of the membrane electrode assembly (MEA), flow field and current collectors, fuel delivery through porous media, and vapor feed via heat recovery from DMFCs [3–7]. Active fuel feed is the primary design for DMFC applications because the fuel circulation system is easier to control. In an active DMFC, a liquid pump such as a squirrel pump, HPLC micropump, or other type of pump must be adopted [8–11]. However, the power consumption of the pumps is up to a few watts and is difficult to integrate into small portable DMFCs, which generate only a few watts of power. Therefore, a low power micropump for DMFC applications would be attractive. Zhang and Wang [12] presented a valveless piezoelectric micropump in a miniaturized DMFC. Even though the total power consumption of the micropump was low, around 70 mW, the required operation voltage of 100 V was still very high for portable DMFCs that operate in the low power (few watts) range. Kim et al. [13] developed a continuous peristaltic magnetic fluid (MF) micropump, which was fabricated using MEMS technology. In their experiments, the input current of their micropump was around 100–600 mA. The maximum flow rate of their microp-

* Corresponding author at: Department of Refrigeration, Air-Conditioning and Energy Engineering, National Chin-Yi University of Technology, No. 35, Lane 215, Section 1, Chung-Shan Road, Taiping Dist., 411 Taichung City, Taiwan.
Tel.: +886 4 23924505x8256; fax: +886 4 23932758.
E-mail addresses: ydkuan@ncut.edu.tw, c699611@yahoo.com (Y.-D. Kuan).

0378-7753/$ – see front matter © 2011 Elsevier B.V. All rights reserved.
doi:10.1016/j.jpowsour.2011.04.060

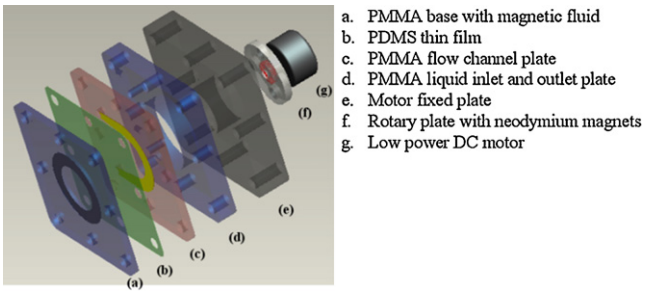

Fig. 1. Exploded view of the 1st MF micropump.

ump was 2.8 μl min^{-1} at 4 rpm and 3.8 μl min^{-1} at 8 rpm, which is quite low for DMFC applications. Shen et al. [14] presented a high-efficiency and self-priming active-valve micropump consisting of a microfluidic chamber structure in glass, which was assembled with a PDMS elastic sheet. This micropump used arc-shaped permanent magnets mounted on the rotational axis of the DC minimotor in a six-phase configuration, which allowed low voltage (0.7 V) and low power (a few tens of milliwatts) operation of the micropump. The flow rate was 2.4 mL min^{-1} at a resonance frequency of around 12 Hz. Hsu et al. [15] demonstrated the fabrication of a peristaltic diffusion-type micropump on polymethylmethacrylate (PMMA) substrates. The maximum flow rate of their micropump was 114.8 μl min^{-1} at a driving frequency of 400 Hz and driving voltage of 100 V. The driving voltage is also quite high for DMFC usage in low power portable applications.

This study will develop a MF micropump, which modifies the characteristics of the micropumps described above and is more suitable for low-power-range DMFCs applications. The proposed micropump has the main advantages of low operation voltage and current, easy fabrication, low cost, and high rigidity, which can potentially allow for mass production of DMFC applications. In this research, two prototype micropumps were designed and fabricated. The prototype micropumps were also applied to feeding methanol fuel to a single cell DMFC test fixture, and the cell performance was measured and compared with the fuel fed by a conventional squirm pump.

2. Design and fabrication of the MF micropumps

2.1. 1st MF micropump

The 1st MF micropump was a prototype for the feasibility study. The exploded view of the first MF micropump is shown in Fig. 1. The poly(methyl methacrylate) (PMMA) base contained 5 cc of magnetic fluid inside a ringed groove. A (PDMS) thin film covered the PMMA substrate. Above the thin film, there was a PMMA plate with a grooved flow channel for transporting the liquid. A PMMA plate with two drilled holes was attached to the flow channel substrate for liquid inlet and outlet to the flow channel substrate. At the top, a low-power DC motor was adopted, and the end of the motor spindle was fixed to a rotary plate, which had neodymium magnets. The DC motor was attached to a motor fixed plate. All components were then screwed together. A complete picture of the first MF micropump is shown in Fig. 2. The main fabrication process of the 1st MF micropump is briefly described as follows. First, the shapes, holes, or grooves of the PMMA related components were milled or drilled using a CNC milling machine. The PDMS thin film was made by adding 10 g of PDMS colloidal solution to the center of a rotating circular glass plate in a spin coater and baking the plate in a vacuum dry oven for 1 h at 75 °C. After the PDMS thin film was fabricated, it was taken out of the vacuum dry oven and cut into several pieces with a predesigned shape. Then, some

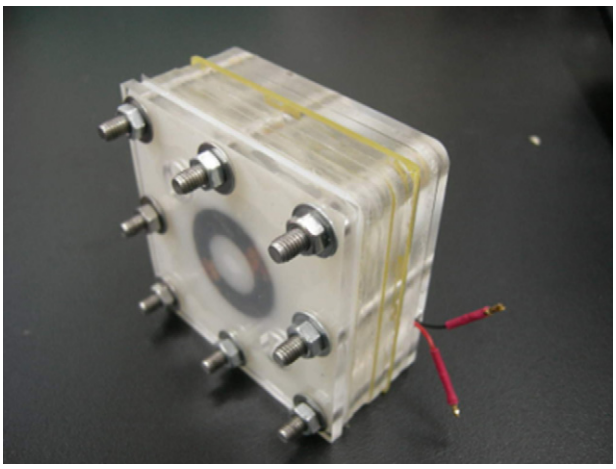

Fig. 2. Picture of the 1st MF micropump.

PDMS colloidal solution was used to coat the surface of the circular groove side of the base with a magnetic fluid and surface of the flow channel side of the flow channel substrate. After injecting 5 cc of magnetic fluid into the circular groove of the base, the PDMS thin film, base with magnetic fluid, and flow channel substrate were bonded at 75 °C and baked for 1 h inside a vacuum dry oven. The last step was to assemble and screw all of the components together.

2.2. 2nd MF micropump

After confirming the feasibility of the 1st MF micropump, the 2nd micropump was designed and developed to reduce the size of the pump. In addition, the structure of the 2nd MF micropump eliminated the screws from the first design. The exploded view of the 2nd MF micropump is shown in Fig. 3. A polypropylene (PP) base contained 2 cc of magnetic fluid inside a circular groove. A PDMS thin film covered the PMMA substrate. Above the thin film, there was a PMMA substrate with a grooved flow channel for transporting liquid, and it also contained the flow inlet and outlet. At the top, a DC motor was attached to a motor fixed base, and the end of the motor shaft was fixed to a rotary plate, which included neodymium magnets. All components were then bonded together. The complete picture of the 2nd MF micropump is shown in Fig. 4. The main fabrication process of the 2nd MF micropump is briefly described as follows. First, the shapes, holes, or grooves of the PMMA and PP components were milled or drilled using a CNC milling machine. The PDMS thin film was made by adding 10 g of PDMS colloidal solution to the center of a rotating circular glass plate on a spin coater and then baking the plate in a vacuum dry oven for 1 h at

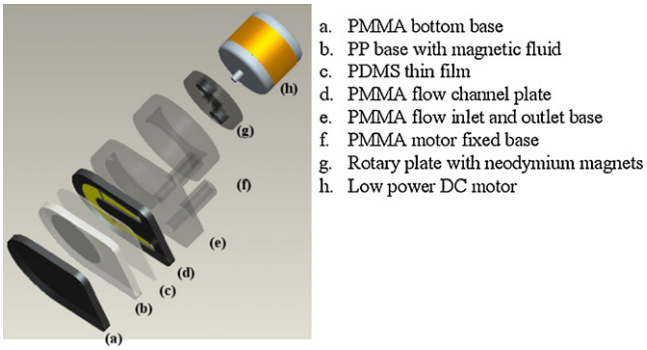

Fig. 3. Exploded view of the 2nd MF micropump.

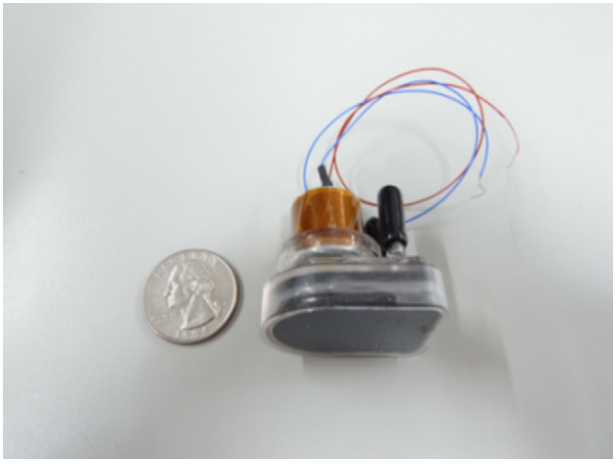

Fig. 4. Picture of the 2nd MF micropump.

75 °C. After the PDMS thin film was fabricated, it was taken out of the vacuum dry oven and cut into several pieces with a predesigned shape. Then, some PDMS colloidal solution was used to coat the surface of the circular groove side of the base with magnetic fluid and surface of the flow channel side of the flow channel substrate. After injecting 2 cc of magnetic fluid into the circular groove of the base, the PDMS thin film, base with magnetic fluid, and flow channel substrate were bonded at 75 °C and baked for 1 h inside a vacuum dry oven. Then, some epoxy glue was spread on the surfaces between the two components. The last step was to assemble and bond all components together.

2.3. Operation mechanisms of the MF micropumps

The operation mechanisms of the 1st and 2nd MF micropumps are the same. The illustration of the operation mechanism of the 1st MF micropump is shown in Fig. 5, and the 2nd MF micropump is shown in Fig. 6. When providing a low DC power to the low-power DC motor, the shaft will rotate and drive the rotation of the rotary disc. The rotary disc contains two or more neodymium magnets. The neodymium magnets will attract the magnetic fluid along with the rotating path. When the rotating neodymium magnets are attracted to each other, the corresponding places of the PDMS thin film will be compressed in sequence such that flow can be pushed forward.

3. Experimental setup

The schematic illustration of the experimental setup is shown in Fig. 7. A beaker, preheated by a temperature-controllable water

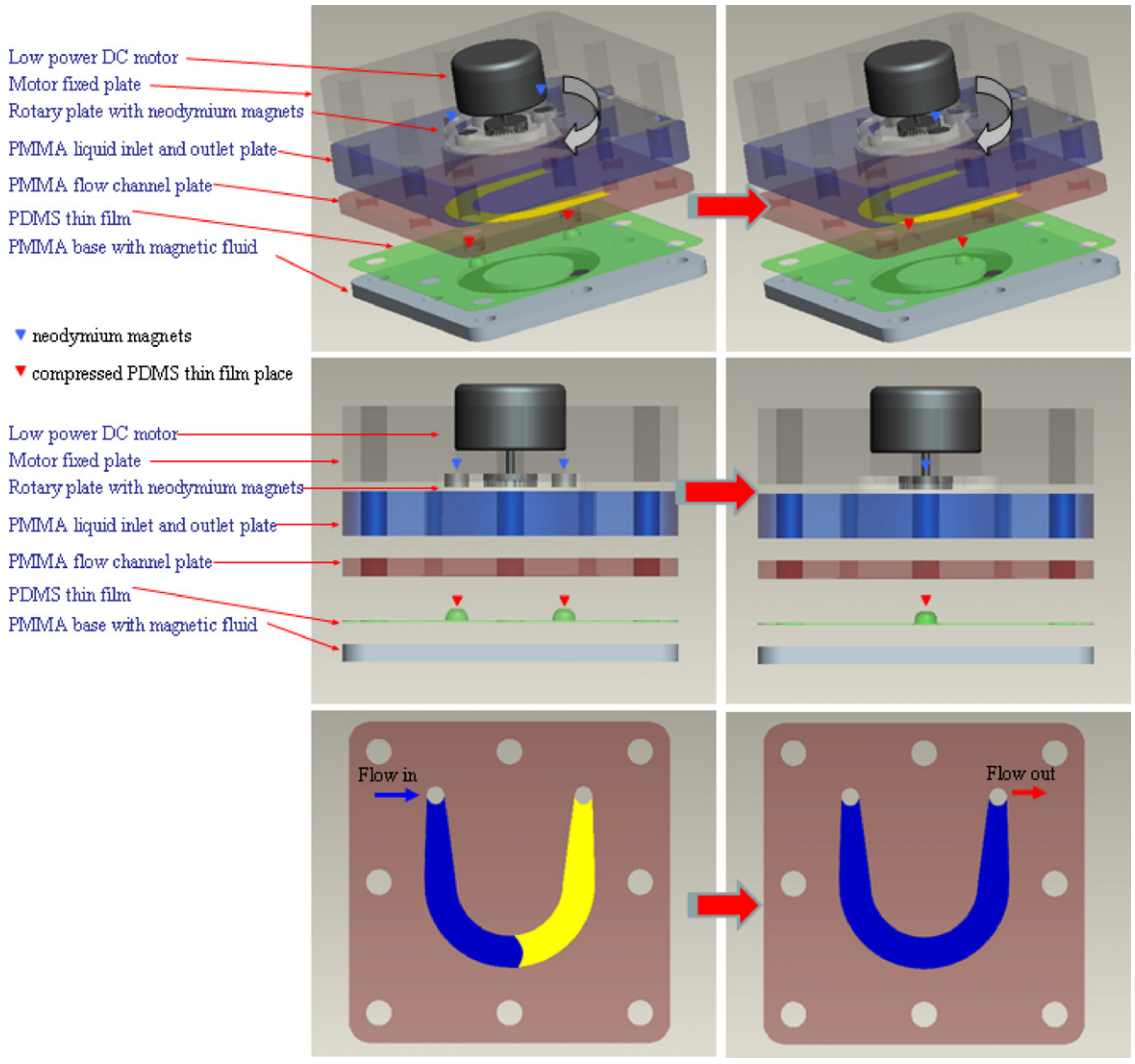

Fig. 5. Illustration of the operation mechanism of the 1st MF micropump.

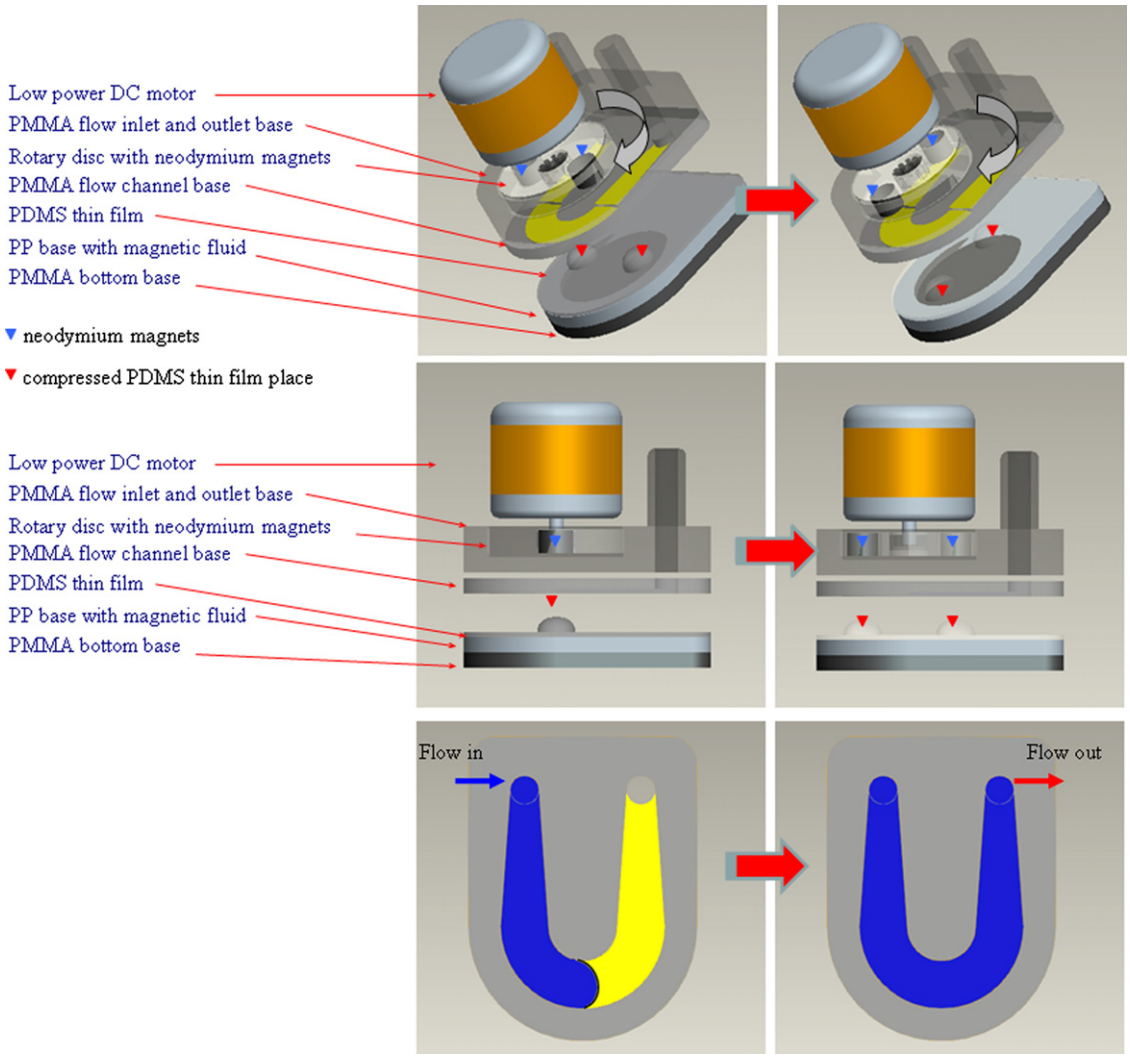

Fig. 6. Illustration of the operation mechanism of the 2nd MF micropump.

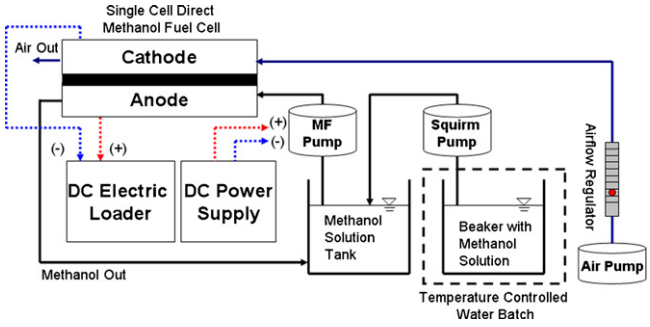

Fig. 7. Schematic illustration of the experimental setup.

bath, contained the methanol solution. The methanol solution was pumped into a methanol solution tank by a squirm pump and kept at a specified temperature. Then, the methanol solution was further pumped into the DMFC anode by the MF micropump. The MF micropump was powered by a DC power supply. The airflow was driven and pumped into the DMFC cathode by an air pump with an airflow regulator. The DMFC was loaded by a DC electric loader to measure the polarization curves of the DMFC.

A single cell DMFC was adopted in the experiment. The membrane electrolyte assembly (MEA) was sandwiched between the anode and cathode current collectors. Nafion® 117 was used as the electrolyte and carbon cloth for the diffusion layers, and the reaction area of the MEA was 35 mm × 35 mm. The catalyst load at the anode was 4 mg cm^{-2} Pt–Ru, and the catalyst load at the cathode was 4 mg cm^{-2} Pt. The current collectors of the DMFC were made of stainless steel 316L (SS316L). Both the anode and the cathode flow boards were made of polymethylmethacrylate (PMMA) and attached to the two end sides of the DMFC test fixture. Each anode and cathode flow board had a single, grooved, serpentine flow channel on its surface.

4. Results and discussion

The DMFC was tested in the laboratory, and the environmental temperature was set to around 25 °C. The concentration of the methanol solution was kept at 2 M. The methanol solution in the methanol solution tank was set to 55 °C.

4.1. Flow rate tests

To determine the characteristics of the MF pumps, experiments on the flow rate of the MF pumps were conducted. The flow outlet of the MF pump was connected to the anode inlet of the DMFC.

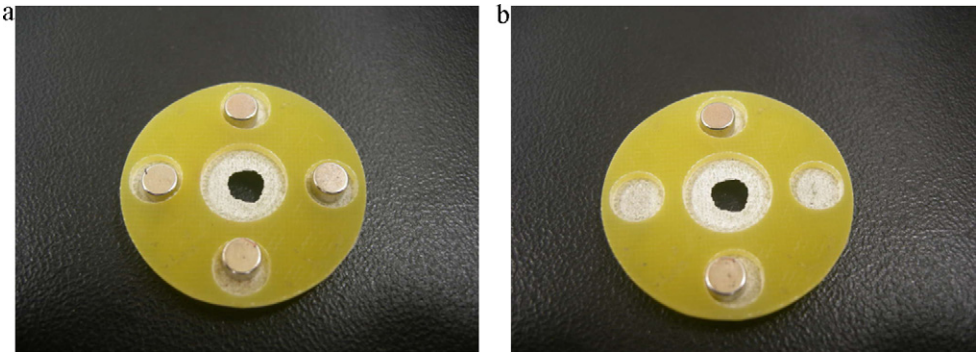

Fig. 8. (a) The rotary disc with two neodymium magnets of the 1st MF micropump. (b) The rotary disc with four neodymium magnets of the 1st MF micropump.

Table 1
The power consumption of the 1st MF micropump (rotary disc with two neodymium magnets).

Voltage (V)	Current (A)	Power (W)
0.7	0.02	0.014
0.8	0.02	0.016
0.9	0.02	0.018
1.0	0.02	0.020
1.1	0.02	0.022
1.2	0.03	0.036
1.3	0.03	0.039
1.4	0.03	0.042

Table 2
The power consumption of the 1st MF micropump (rotary disc with four neodymium magnets).

Voltage (V)	Current (A)	Power (W)
0.7	0.02	0.014
0.8	0.02	0.016
0.9	0.03	0.027
1.0	0.04	0.040
1.1	0.04	0.044
1.2	0.04	0.048
1.3	0.04	0.052
1.4	0.04	0.056

In the 1st MF pump, the rotary disc had two or four neodymium magnets, as shown in Fig. 8a and b. The power consumptions of the rotary disc with two neodymium magnets under a 0.7–1.4 V operating voltage range are listed in Table 1. The results show that the operating currents were 0.02–0.03 A in different ranges, and the power consumptions were low (0.014–0.042 W). The flow rates of the methanol solution under different operating voltages are shown in Fig. 9. The flow rate increased with increasing operating voltage until 1.2 V, and the average maximum flow rate was 7.2 cc min^{-1}. Further increasing the operating voltage would decrease the flow rate. The power consumptions of the rotary disc with four neodymium magnets under a 0.7–1.4 V operating voltage range are listed in Table 2. The results show that the operating currents were 0.02–0.04 A under different ranges, and the power consumptions were low (0.014–0.056 W). The flow rates of the methanol solution under different operating voltages are shown in Fig. 10. The flow rate increased with increasing operating voltage until 1.0 V, and the average maximum flow rate was 5.5 cc min^{-1}. Further increasing the operating voltage decreased the flow rate.

The power consumption of the rotary consumption with four neodymium magnets was higher than the one with two neodymium magnets because the rotary with four neodymium magnets is heavier than the one with two neodymium magnets, such that the DC motor requires higher power to drive the

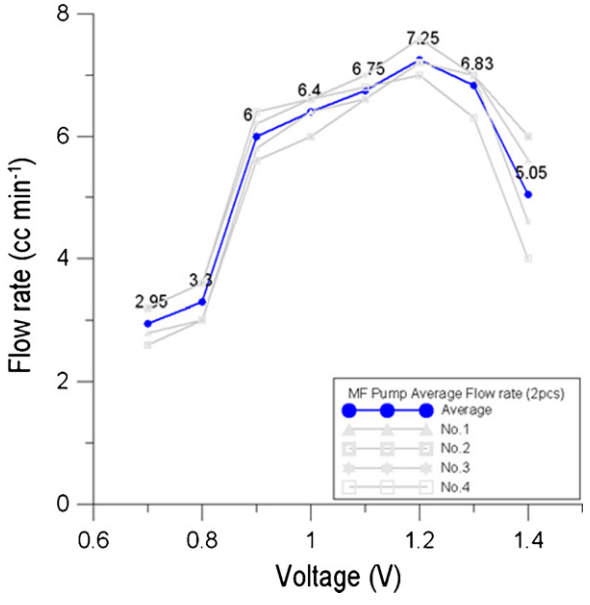

Fig. 9. The flow rates of the methanol solution under different operating voltages by the 1st MF micropump, in which the rotary disc contains two neodymium magnets.

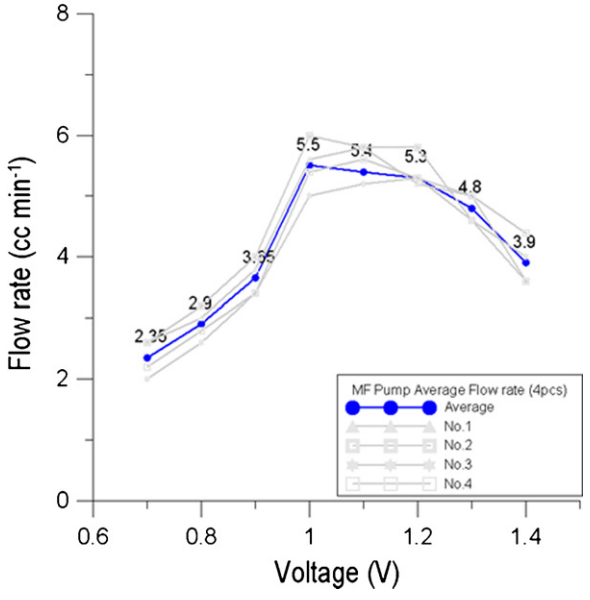

Fig. 10. The flow rates of the methanol solution under different operating voltages by the 1st MF micropump, in which the rotary disc contains four neodymium magnets.

Table 3
The power consumption of the 2nd MF micropump (rotary disc with two neodymium magnets).

Voltage (V)	Current (A)	Power (W)
0.7	0.02	0.014
0.8	0.03	0.024
0.9	0.03	0.027
1.0	0.03	0.030
1.1	0.03	0.033
1.2	0.03	0.036
1.3	0.03	0.039
1.4	0.03	0.042

rotary disc. In addition, the flow rate of the rotary disc with two neodymium magnets was higher than the one with four neodymium magnets because the rotary with two neodymium magnets had a larger space for the passage of liquid as compared to the rotary disc with four neodymium magnets when pumping the liquid.

Based on the results of the flow rate tests, the rotary disc of the 2nd MF pump directly adopts two neodymium magnets for the rotary disc. The power consumptions of the rotary disc with two neodymium magnets under a 0.7–1.4 V operating voltage range are listed in Table 3. The results show that the operating currents were 0.02–0.03 A under different ranges, and the power consumptions were low (0.014–0.042 W). The flow rates of the methanol solution under different operating voltages are shown in Fig. 11. The flow rate increased with increasing operating voltage until 0.8 V, and the average maximum flow rate was 6.9 cc min^{-1}. Further increasing the operating voltage decreased the flow rate.

In addition, the MF micropump might not yield a higher flow rate with increasing operating voltage because of the following reasons. The rotation speed of the rotary disc will increase with higher operating voltage, such that the time for the neodymium magnet to attract the magnet fluid becomes shorter, and the protruded highs at the thin film along with the rotating neodymium magnets become lower. Although the higher rotating speed of the rotary disc will lead to a higher frequency of fluid pushing and increase the flow rate, the lower protruded highs will decrease the fluid pumping force and lead to a lower flow rate. Therefore, there

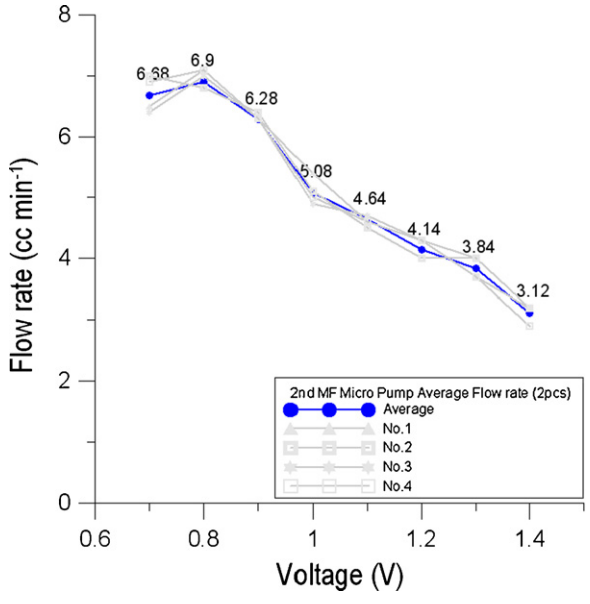

Fig. 11. The flow rates of the methanol solution under different operating voltages by the 2nd MF micropump, in which the rotary disc contains four neodymium magnets.

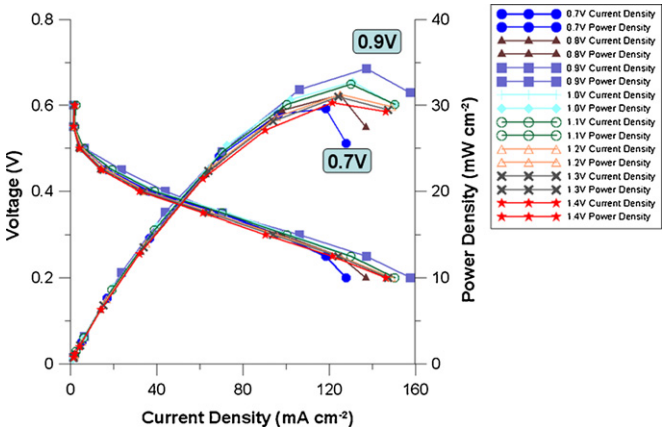

Fig. 12. The DMFC performance curves under different operating voltages of the 1st MF micropump.

exists an optimal operating voltage that results in the highest flow rate for each MF micropump.

4.2. DMFC performance tests

Because the MF micropumps in this paper were designed for DMFC usage, the MF micropumps were connected to a DMFC to pump the anode methanol solution, and DMFC performance tests were then conducted to demonstrate system feasibility. Both of the rotary discs of the MF micropumps contained two neodymium magnets. The DMFC performance curves under different operating voltages for the 1st MF micropump are shown in Fig. 12. The 0.7 V operating voltage of the 1st MF micropump yielded the lowest DMFC cell performance and the 0.9 V operating voltage yielded the highest DMFC cell performance. The DMFC performance curves under different operating voltages for the 2nd MF micropump are shown in Fig. 13. The 1.4 V operating voltage of the 2nd MF micropump yielded the lowest DMFC cell performance, and the 0.9 V operating voltage yielded the highest DMFC cell performance. The corresponding liquid flow rate at 0.9 V operating voltage for the 1st MF micropump was 6 cc min^{-1}. The corresponding liquid flow rate at 0.9 V operating voltage for the 2nd micropump is 6.2 cc min^{-1}, which is similar to that of the 1st MF micropump. The power consumptions of the MF micropumps are in the range of dozens of milliwatts, and therefore, the very power consumption demonstrates the feasibility of the proposed MF micropumps for DMFC applications.

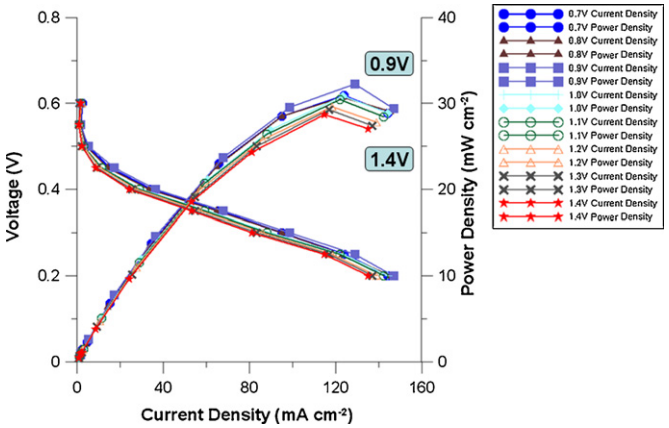

Fig. 13. The DMFC performance curves under different operating voltages of the 2nd MF micropump.

5. Conclusions

This paper presented a type of magnetic fluid micropump for DMFC applications that has specific characteristics of low operating voltage and current. The design and fabrication processes and mechanism of operation were described in detail. Two prototypes were successfully developed. The 1st MF micropump was built as a proof of concept. The 2nd micropump was designed and fabricated to reduce the size of the 1st MF micropump. Based on the discussion, the rotary disc with two neodymium magnets is better than that with four neodymium magnets. Based on these results, the current required for the 1st MF micropump (the rotary disc with two neodymium magnets) was only 0.02–0.03 A for operating voltages of 0.7–1.4 V. The resulting liquid flow rate was about 2.95–7.25 cc min^{-1}. The current required for the 2nd MF micropump (the rotary disc with two neodymium magnets) was only 0.02–0.03 A for operating voltages of 0.7–1.4 V. Here, the resulting liquid flow rate was approximately 3.12–6.9 cc min^{-1}. DMFC performance tests were also conducted by pumping the anode fuel into the DMFC with the proposed MF micropumps. The results showed the feasibility of the MF micropumps for future DMFC applications. Further durability tests of the MF micropumps will need to be conducted to ensure that the system is suitable for long-term deployment.

Acknowledgements

The authors would like to acknowledge financial supports from the National Science Council of Taiwan, ROC (NSC 99-2221-E-167-017-MY2 and NSC 100-3113-E-167-001) and the National Nano Device Laboratories of Taiwan, ROC (NDL99-C06M2G-063).

References

[1] J. Larminie, A. Dicks, Fuel Cell Systems Explained, 2nd ed., John Wiley & Sons Ltd., West Sussex, England, 2003.
[2] R. O'Hayre, S.-W. Cha, W. Colella, F.B. Prinz, Fuel Cell Fundamentals, John Wiley & Sons Inc., NY, USA, 2006.
[3] M.A. Abdelkareem, N. Morohashi, N. Nakagawa, Journal of Power Sources 172 (2007) 659–665.
[4] A. Faghri, Z. Guo, Applied Thermal Engineering 28 (2008) 1614–1622.
[5] Z. Guo, A. Faghri, International Communications in Heat and Mass Transfer 35 (2008) 225–239.
[6] C.H. Lee, C.H. Park, S.Y. Lee, B.O. Jung, Y.M. Lee, Desalination 233 (2008) 210–217.
[7] M.A. Abdelkareem, T. Tsujiguchi, N. Nakagawa, Journal of Power Sources 195 (2010) 6287–6293.
[8] Y.-D. Kuan, S.-M. Lee, M.-F. Sung, Journal of Fuel Cell Science and Technology 6 (2009) 011004-1–011004-9.
[9] Y.-D. Kuan, J.-Y. Chang, S.-M. Lee, S.-R. Lee, Journal of Power Sources 187 (2009) 112–122.
[10] H. Yang, T.S. Zhao, Electrochimica Acta 50 (2005) 3243–3252.
[11] C.Y. Chen, D.H. Liu, C.L. Huang, C.L. Chang, Journal of Power Sources 167 (2007) 442–449.
[12] T. Zhang, Q.-M. Wang, Journal of Power Sources 140 (2005) 72–80.
[13] E.-G. Kim, J.-G. Oh, B. Choi, Sensors and Actuators A: Physical 128 (2006) 43–51.
[14] M. Shen, L. Dovat, M.A.M. Gijs, Sensors and Actuators B: Physical (2009), available on line.
[15] Y.-C. Hsu, J.-H. Li, N.-B. Le, Sensors and Actuators A: Physical 148 (2008) 149–157.